

Thermal conductivity of single-crystal Bi-Sr-Ca-Cu-O

M. F. Crommie and A. Zettl

*Department of Physics, University of California at Berkeley, Berkeley, California 94720
and Materials and Chemical Sciences Division of the Lawrence Berkeley Laboratory, Berkeley, California 94720*

(Received 30 January 1990)

The *ab*-plane thermal conductivity κ of single-crystal $\text{Bi}_2\text{Sr}_2\text{CaCu}_2\text{O}_{8-x}$ has been measured from 25 to 300 K, for samples of varying oxygen configuration. Complementary electrical-conductivity measurements on the same crystals allow κ to be accurately decomposed into electronic and phonon contributions. For metallic samples the electronic contribution to κ is substantial. Analysis of κ in the normal and superconducting states allows the defect-scattering and electron-scattering contributions to κ_{phonon} to be evaluated near T_c . κ in the superconducting state is consistent with a BCS description.

Understanding the normal-state properties and superconductivity mechanism in high-temperature superconductors (HTSC's) is a challenging problem. Transport measurements such as electrical resistivity, thermopower, and Hall effect are valuable in establishing normal-state interactions and parameters.¹ In the HTSC $\text{Bi}_2\text{Sr}_2\text{CaCu}_2\text{O}_{8-x}$ (Bi-Sr-Ca-Cu-O), for example, recent transport experiments have demonstrated an anisotropic electronic structure highly sensitive to the oxygen configuration, with a possibly important role played by defect scattering.^{2,3}

The thermal conductivity κ is a particularly useful transport coefficient in that it can probe scattering processes in both the normal state and the superconducting state below T_c . Previous measurements of κ in polycrystalline Bi-Sr-Ca-Cu-O (Ref. 4) have demonstrated a bumplike structure just below T_c , similar to that observed in other HTSC materials⁵⁻⁸ and interpreted as due to enhancement of the phonon contribution resulting from a reduction of phonon-electron scattering. However, using polycrystalline data, a quantitative deconvolution of κ into its intrinsic electronic and phonon contributions is difficult due to the complexity of the polycrystalline system.

We here report measurements of the thermal conductivity of single crystal Bi-Sr-Ca-Cu-O in the important temperature range from room temperature to below T_c . The measurements were performed along the *ab* plane for crystals with different oxygen configuration. In contrast to polycrystalline measurements,⁴⁻⁷ we find that, for oxygen-rich samples in the normal state, the electronic portion of κ is comparable to the phonon contribution. By analyzing κ in the superconducting state, we further deconvolve the phonon thermal resistivity at T_c into its distinct electron- and defect-scattering components. Our results are generally consistent with a κ determined from BCS theory.

Bi-Sr-Ca-Cu-O crystals were prepared as described elsewhere.⁹ The crystals were cleaved into thin *ab*-plane sheets of typical dimension $2 \times 1 \times 0.01$ mm³. The oxygen configuration of the crystals was altered by annealing in

either oxygen (samples *A* and *B*) or a vacuum (samples *C* and *D*), using the same procedure employed in other Bi-Sr-Ca-Cu-O transport studies.^{2,3} The thermal conductivity was measured using a steady-state comparative technique,¹⁰ where a constantan wire attached in series with the sample served as a calibrated heat link. Since the thermal conductivity of the constantan enters the analysis, we determined, using an independent Joule heating method, the absolute (temperature-dependent) thermal conductivity of the constantan; good agreement with published results¹¹ was obtained. Average temperature gradients across the sample were 0.5 K, and error due to radiation and heat leaks through the wires was estimated to be only a few percent. Although the absolute κ measured for the samples has a potentially large error due to uncertainties in the effective sample geometry, such errors largely cancel out in our analysis where the electrical conductivity, σ (measured on the same crystal with similarly placed leads) is used. The error in κ/σ is small, $\leq 5\%$.

Figure 1(a) shows the temperature dependence of the measured *ab*-plane thermal conductivity, $\kappa_m(T)$, for samples *A* and *B*. The data have the same qualitative shape as polycrystalline results.⁴ For both samples κ_m decreases almost linearly with decreasing temperature until $T_c \approx 89$ K. Below T_c , κ_m increases and reaches a local maximum at $T \approx 62$ K; below this temperature κ_m decreases rapidly. Figure 1(b) shows the electrical resistivity $\rho(T)$ [$=1/\sigma(T)$] for samples *A* and *B*. The form of $\rho(T)$ is suggestive of "metallic" behavior, characteristic of Bi-Sr-Ca-Cu-O samples having undergone a high oxygen anneal.² The electrical resistivity data indicate onset to the superconducting transition at $T_c \approx 89$ K and $\rho=0$ at $T_{cf} \approx 81$ K.

Figure 2 shows similar $\kappa_m(T)$ and $\rho(T)$ data for samples *C* and *D*. These samples were processed using a low oxygen anneal, and, as seen in Fig. 2(b), do not display metallic behavior in the electrical resistivity. Rather, these samples have room-temperature electrical resistivities an order of magnitude higher than those of samples

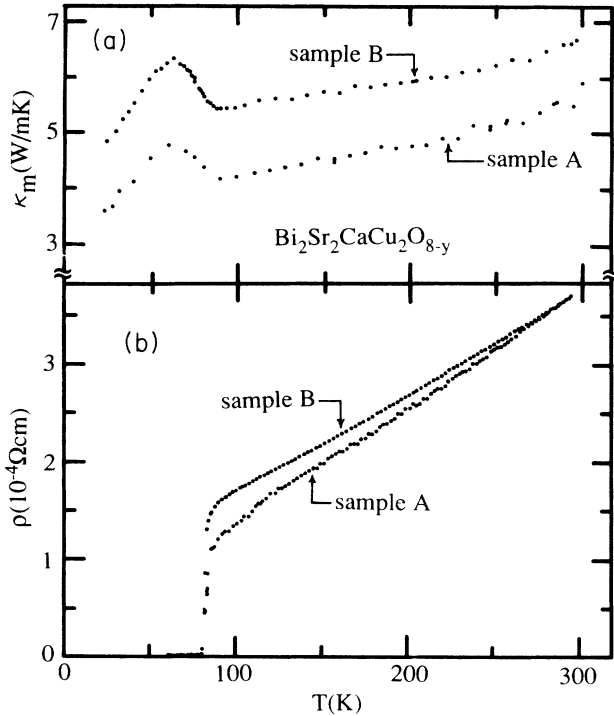


FIG. 1. (a) Measured ab -plane thermal conductivity vs temperature for two metallic crystals of $\text{Bi}_2\text{Sr}_2\text{CaCu}_2\text{O}_{8-y}$. (b) ab -plane resistivity vs temperature for the same two crystals.

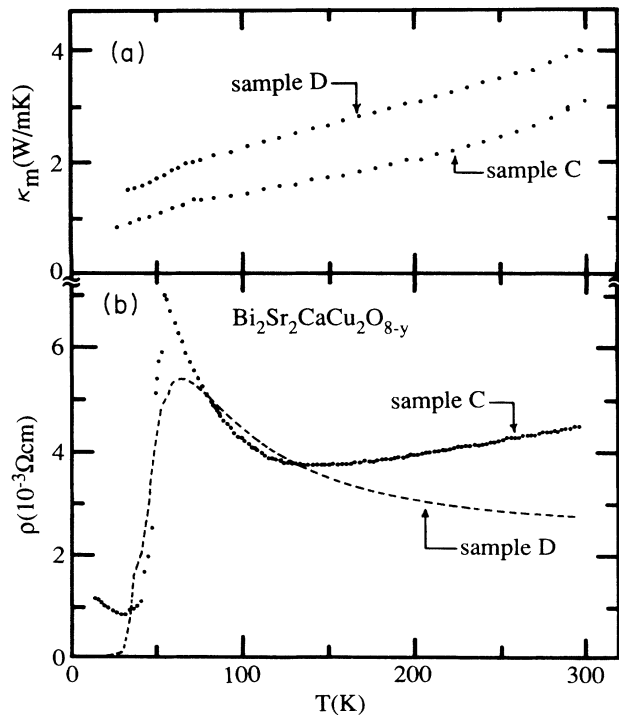


FIG. 2. (a) Measured ab -plane thermal conductivity for two nonmetallic oxygen-deficient crystals of $\text{Bi}_2\text{Sr}_2\text{CaCu}_2\text{O}_{8-y}$. (b) ab -plane resistivity vs temperature for the same two crystals.

A and B , and both show the characteristic semiconductorlike upturn in $\rho(T)$ before ρ drops at the severely depressed $T_c \approx 55$ K. The κ_m for samples C and D again varies nearly linearly with temperature (with a positive slope slightly larger than for the metallic samples A and B). Unlike the metallic samples, the oxygen-deficient samples C and D show no upturn in κ_m either at $T = 89$ K or their own depressed $T_c \approx 55$ K, i.e., the “bump” anomaly is fully absent. The only notable feature of the κ_m data for samples C and D is a downward “kink” near 60 K. It is not clear if this kink is due to the onset of superconductivity in these samples ($T_c \approx 55$ K), or if it corresponds to the same sharp downturn in κ_m near 62 K observed in the metallic samples A and B and represents, for example, an intrinsic scattering mechanism such as defects (it is unlikely to be due to boundary scattering). If the latter case is true, then this implies that the gross defect structure within the two differently treated crystals is similar.

It is noteworthy that the magnitude of κ_m for samples C and D is approximately one-half that of the metallic samples A and B . This demonstrates that removing electrical carriers from the sample reduces the thermal conductivity, which suggests that in the normal state above T_c , the electrons in metallic samples carry a significant portion of the heat.

We now analyze our κ_m data for the metallic Bi-Sr-Ca-Cu-O samples A and B , making use of the corresponding electrical-conductivity data. The electronic and phonon contributions to κ_m in the normal state are most directly obtained from the Wiedemann-Franz (WF) law. Figure 3(a) shows the measured Lorenz ratio, $L(T) = \kappa_m(T)/\sigma(T)T$, for samples A and B . As mentioned before, geometrical uncertainties cancel here. The magnitude of the Lorenz ratio for the metallic samples is roughly three times the Sommerfeld value, $L_0 = 2.45 \times 10^{-8} \text{ W } \Omega / \text{ K}^2$. Since $\rho(T)$ is roughly linear in temperature for metallic Bi-Sr-Ca-Cu-O, the upward curvature in the Lorenz ratio for sample B is mostly due to the impurity offset in electrical resistivity of that sample. Assuming the validity of the WF law for the metallic samples, the data of Fig. 3(a) imply that roughly one-third of the thermal conductivity is due to electrons, while phonons make up the rest. This result is at odds with most polycrystalline data, which has been interpreted as implying that the electrons carry only 1–12% of the heat in the HTSC's.^{4–7} Our result is similar to findings for single-crystal $\text{YBa}_2\text{Cu}_3\text{O}_7$ where electrons appear to carry $\sim 55\%$ of the heat¹² (again contrary to polycrystalline data interpretations).

The Lorenz ratio for the oxygen-deficient samples C and D is shown in Fig. 3(b). Here $L \approx 20L_0$ at higher temperature (200–300 K) and increases with decreasing temperature. If the WF law holds for samples C and D , then the data of Fig. 3(b) imply that electrons carry less than 5% of the heat in oxygen-deficient Bi-Sr-Ca-Cu-O, while phonons account for the rest.

Figure 4 shows the results of the first step in a quantitative deconvolution of the thermal conductivity into its different carrier and scattering components. Here the measured thermal conductivity $\kappa_m(T)$ along with its con-

stituent electron and phonon components $\kappa_e(T)$ and $\kappa_p(T)$ is shown for the two metallic samples. Combining the WF law with the assumption

$$\kappa_m(T) = \kappa_e(T) + \kappa_p(T) \quad (1)$$

leads to

$$\kappa_p(T) = \kappa_m(T) - L_0 \sigma(T) T. \quad (2)$$

Implicit in the use of the WF law is the assumption that the thermal resistance is dominated by large-angle "horizontal" scattering events.¹³ If small-angle "vertical" events are significant, then $\kappa_e(T) < L_0 \sigma(T) T$ and $\kappa_m(T) - L_0 \sigma(T) T$ is a lower bound for $\kappa_p(T)$. Figure 4 shows explicitly that the thermal conductivity of metallic Bi-Sr-Ca-Cu-O is in the complicated regime where neither the electrons nor the phonons fully dominate the heat transport. We note that the quantitative subtraction in Eq. (2) is possible only if both $\kappa_m(T)$ and $\sigma(T)$ are measured on the *same* crystal (which is the case here), which minimizes geometrical error and allows the derived $\kappa_e(T)$ to reflect the unique defect configuration of the particular sample being measured for $\kappa_m(T)$. The large electronic contribution to κ_m suggests that calculations which ignore κ_e (such as those¹⁴ used to extract values of λ from polycrystalline thermal conductivity data) are inadequate for single-crystal Bi-Sr-Ca-Cu-O (or $\text{YBa}_2\text{Cu}_3\text{O}_7$).

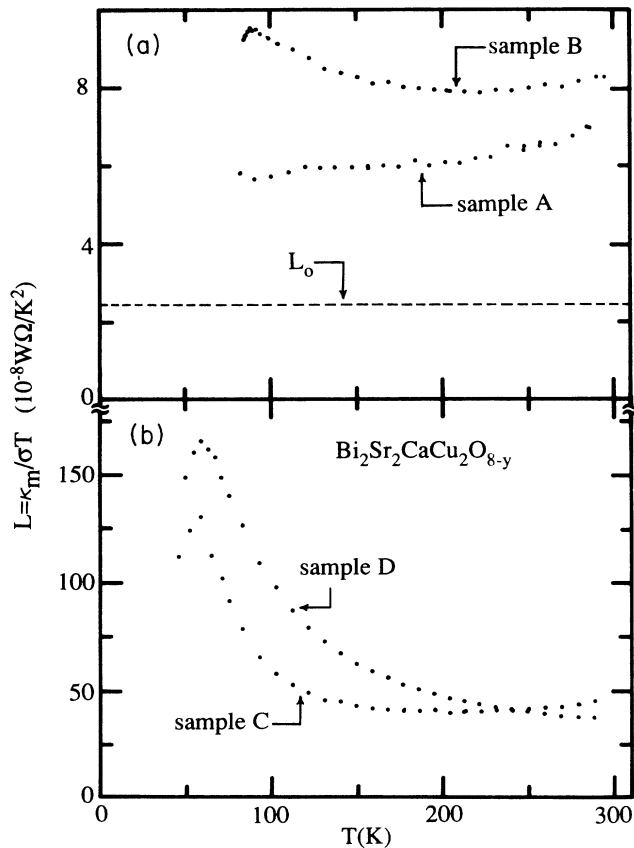


FIG. 3. *ab*-plane Lorenz ratio, $L = \kappa_m / \sigma T$, for (a) the two metallic crystals shown in Fig. 1 (the Sommerfeld value, $L_0 = 2.45 \times 10^{-8} \text{ W}\Omega/\text{K}^2$, is included for comparison) and (b) the two nonmetallic, oxygen-deficient crystals shown in Fig. 2.

It is desirable to separate the phonon thermal conductivity into its defect and electronic scattering components. To do this we use κ data for metallic Bi-Sr-Ca-Cu-O samples from both the normal and superconducting states. From Mathiessens's rule the phonon thermal resistivity may be written as the sum of the thermal resistivity due to electrons and that due to defects:

$$1/\kappa_p(T) = W_p^e(T) + W_p^d(T). \quad (3)$$

Phonon-phonon umklapp processes are ignored, as they are likely overshadowed by scattering from the defects and electrons. (This assumption is supported by data on the oxygen-deficient samples shown in Fig. 2, where κ_m is dominated by phonons, but nowhere does it have the region of negative slope that one might expect if umklapp scattering were important. We also note that the umklapp processes freeze-out at lower temperatures. The temperature dependence of the thermal conductivity of the oxygen-deficient samples thus implies that it is dominated by phonon-defect scattering.)

In the normal state $\kappa_p(T)$ for Eq. (3) is known from Eq. (2), but Eq. (2) is no longer valid in the superconducting state. There the temperature dependence of the phonon and electron components are modified by the opening of the superconducting energy gap. The thermal conductivity due to quasiparticles in the superconducting state has been studied for weak-coupling BCS superconductors

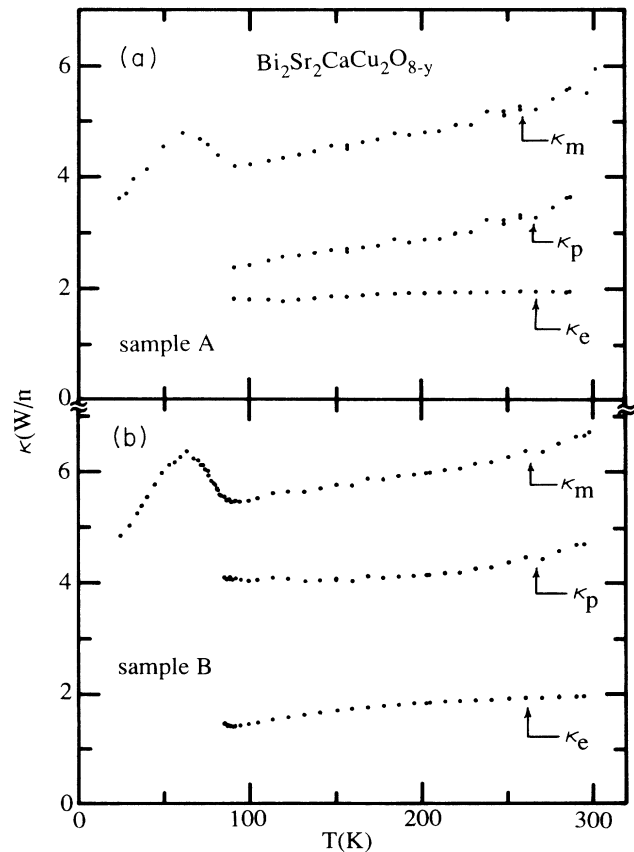


FIG. 4. Temperature dependence of measured *ab*-plane thermal conductivity κ_m shown with deduced phonon and electron components (κ_p and κ_e) for (a) sample A and (b) sample B.

in the limits where the scattering is dominated by either defects or phonons.¹⁵⁻¹⁷ The strong-coupling regime has been studied for the phonon-limited thermal conduction of quasiparticles when T/T_c is near 1.^{17,18} The thermal conductivity of phonons in weak-coupling superconductors has also been studied theoretically.^{14,15,17} It is convenient to define

$$\beta(T/T_c) = \kappa_e(T)_s / \kappa_e(T)_n$$

and

$$1/k_m(T) = 1/[k_p(T) + k_e(T)] = [W_p^d(T)_n + \alpha W_p^e(T)_n] / \{1 + \beta \kappa_e(T)_n [W_p^d(T)_n + \alpha W_p^e(T)_n]\}, \quad (4)$$

where the assumption has been made that $W_p^d(T)$ (the defect-limited phonon thermal resistivity) does not change appreciably due to the onset of superconductivity. Equation (4) reduces to Eq. (3) for $T \geq T_c$ with aid of the WF law.

It is desirable to solve Eq. (4) for the two parameters $W_p^e(T)$ and $W_p^d(T)$. W_p^d , the thermal resistivity of the phonons due to scattering by defects, provides basic information on the role of defects in the crystal, while W_p^e , the thermal resistivity of the phonons due to scattering by electrons, provides information on the electron-phonon interaction. Equation (4) may be solved for these parameters near T_c using experimental data from the normal and superconducting states (data from the normal state alone leads to more unknown variables than equations). For the normal state we use data from the metallic samples at $T_1 = T_c = 89$ K, the onset of the resistive transition, while for the superconducting state we use data at $T_2 = 62$ K, the maximum of the thermal conductivity below T_c . These temperature points are close enough to justify the approximation that $W_p^e(T)_n$ and $W_p^d(T)_n$ change negligibly in the temperature range $T_1 \geq T \geq T_2$. [The data of Fig. 2(a) on the oxygen-deficient material also help to justify this approximation in regard to $W_p^d(T)_n$]. Evaluating Eq. (3) at T_1 and Eq. (4) at T_2 leads to the following expression for $W_p^e(T_1)$:

$$W_p^e(T_1) = [\kappa_m(T_2) - \kappa_p(T_1) - \beta \kappa_e(T_2)_n] / \{(\alpha - 1) \kappa_p(T_1) [\beta \kappa_e(T_2)_n - \kappa_m(T_2)]\}. \quad (5)$$

$W_p^d(T_1)$ follows directly from Eq. (3). Equation (5) is evaluated using the data shown in Fig. 4 for $\kappa_m(T_2)$ and $\kappa_p(T_1)$, while $\kappa_e(T_2)_n$ is determined by extrapolating the linear resistivity data of Fig. 1 down to T_2 and using the WF law. $\alpha(T_2/T_c = 0.7)^{-1} \approx 10$ in the weak-coupling limit¹⁷ [$\alpha(T/T_c)$ has not, to our knowledge, been calculated in the strong-coupling limit]. $\beta(T_2/T_c)$ is more difficult to obtain since the electron thermal conductivity is not clearly in the defect- or phonon-dominated scattering limit. However, in the weak-coupling regime the two limits yield roughly equivalent values at $T/T_c \approx 0.7$, with $\beta(0.7) \approx 0.7$.¹⁵⁻¹⁷

Our final values of $W_p^e(89$ K) and $W_p^d(89$ K) are then 1.6×10^{-1} and 2.6×10^{-1} K m/W, respectively, for sample *A*, and 8.0×10^{-2} k m/W and 1.7×10^{-1} K m/W, respectively for sample *B*. The defect-scattering component of the phonon thermal resistivity is thus roughly twice the magnitude of the electron-scattering component in the vicinity of T_c , which demonstrates an important role played by the defects.

Our treatment of the thermal conductivity leading to Eqs. (4) and (5) can be examined for self-consistency using the standard transport relation¹³

$$W_p^e(T) \approx [\rho_\lambda(T)/T] (e/k_B)^2 [3N n_a k_B / C_\lambda(T)]^2, \quad (6)$$

where $\rho_\lambda(T)$ is the electrical resistivity due to phonons, N is the total number of atoms (units cells), n_a is the number of charge carriers per atom (unit cell), and C_λ is the lattice heat capacity. Using $W_p^e(T_c)$ obtained above, $\rho_\lambda(T)/T$ obtained from the slope of the measured resis-

$$\alpha(T/T_c)^{-1} = W_p^e(T)_n / W_p^e(T)_s$$

for a BCS superconductor in different scattering and coupling regimes. Here $\kappa_e(T)_s$ is the electron thermal conductivity for a superconducting material at $T < T_c$, while $\kappa_e(T)_n$ is the electron thermal conductivity that same material *would* have if there were no superconductivity present (for instance, if it were placed in a large magnetic field). $W_p^e(T)_s$ and $W_p^e(T)_n$ represent the electron-limited phonon thermal resistivity under analogous conditions. With the preceding definitions of α and β , the total thermal resistivity becomes, for $T < T_c$,

tivity (Fig. 1), and $n_a \approx 1$ as obtained from Hall effect measurements,³ Eq. (6) leads to a lattice specific heat $c_\lambda(89$ K) ≈ 80 J/mol K for sample *A* and $c_\lambda(89$ K) ≈ 110 J/mol K for sample *B* ("mol" refers to the number of unit cells). Unfortunately no direct specific-heat measurements on single-crystal Bi-Sr-Ca-Cu-O have been reported in this temperature range. Our predicted values of c_λ , however, are of similar magnitude to $c_\lambda(89$ K) ≈ 300 J/mol K obtained by direct specific-heat measurements on polycrystalline Bi-Sr-Ca-Cu-O specimens,¹⁹ and thus lend support to the assumptions and approximations made in our analysis.

In conclusion, the normal-state thermal conductivity of Bi-Sr-Ca-Cu-O in the metallic regime has substantial electron and phonon contributions. The behavior in the superconducting state is consistent with conventional BCS behavior and suggests that near T_c the phonon portion of the thermal resistivity has electron- and defect-scattering terms, the defect term being approximately twice as large as the electron-scattering contribution.

We thank Professor M. L. Cohen for helpful discussions, and G. Briceno for growing the crystals used in this study. This work was supported by the Director, Office of Energy Research, Office of Basic Energy Sciences, Materials Sciences Division of the U. S. Department of Energy under Contract No. DE-AC03-76SF00098. M.F.C. acknowledges support from the Department of Education.

- ¹See, for example, *Mechanisms of High Temperature Superconductivity*, edited by H. Kamimura and A. Oshiyama (Springer-Verlag, New York, 1989).
- ²M. F. Crommie *et al.*, Phys. Rev. B **41**, 2526 (1990).
- ³G. Briceno and A. Zettl, Phys. Rev. B **40**, 11 352 (1989).
- ⁴S. D. Peacor and C. Uher, Phys. Rev. B **39**, 11 559 (1989).
- ⁵D. T. Morelli, J. Heremans, and D. E. Swets, Phys. Rev. B **36**, 3917 (1987).
- ⁶C. Uher and A. B. Kaiser, Phys. Rev. B **36**, 5680 (1987).
- ⁷U. Gottwick *et al.*, Europhys. Lett. **4**, 1183 (1987).
- ⁸M. A. Izbizky *et al.*, Phys. Rev. B **38**, 9220 (1988).
- ⁹J.-M. Imer *et al.*, Phys. Rev. Lett. **62**, 336 (1989).
- ¹⁰E. B. Lopes, M. Almeida, J. Dumas, and J. Marcus, Phys. Lett. A **130**, 98 (1988).
- ¹¹R. W. Powers, J. B. Ziegler, and H. L. Johnston, in *Thermophysical Properties of Matter*, edited by Y. S. Touloukian, R. W. Powell, C. Y. Ho, and P. G. Klemens (Plenum, New York, 1970), Vol. 1, p. 566.
- ¹²S. J. Hagen, Z. Z. Wang, and N. P. Ong, Phys. Rev. B **40**, 9389 (1989).
- ¹³J. M. Ziman, *Electrons and Phonons* (Clarendon, Oxford, 1960). [Note that Eq. (6) is in cgs units, whereas the numbers quoted in our paper are in mks units.]
- ¹⁴L. Tewordt and Th. Wolkhausen, Solid State Commun. **70**, 839 (1989).
- ¹⁵J. Bardeen, G. Rickayzen, and L. Tewordt, Phys. Rev. **113**, 982 (1959).
- ¹⁶Ludwig Tewordt, Phys. Rev. **129**, 657 (1963).
- ¹⁷B. T. Gielikman and V. Z. Kresin, *Kinetic and Nonsteady-State Effects in Superconductors* (Wiley, New York, 1974).
- ¹⁸Vinay Ambegaokar and James Woo, Phys. Rev. **139** A1818 (1965).
- ¹⁹R. A. Fisher *et al.*, Phys. Rev. B **38**, 11 942 (1988).